Synthesis, structure and thermal decomposition of tetra(2-pyridyl)pyrazine·I_2 charge-transfer complexes

Rosa D. Bailey,[a] M. Grabarczyk,[b] T. W. Hanks*,[b] and William T. Pennington*,[b]

[a] *Department of Chemistry, Hunter Chemistry Laboratories, Clemson University, Clemson, SC 29631, USA*

[b] *Department of Chemistry, Furman University, Greenville, SC 29613, USA*

In both the solid state and in solution, 2,3,5,6-tetrakis(2′-pyridyl)pyrazine (tpp) reacts with iodine to form charge-transfer complexes. The solid state process results in the exclusive production of a mono-I_2 adduct, 3, while the solution reaction can produce both 3 and a bis-I_2 adduct, 4. The X-ray crystal structure of 4 is described and a structure for 3 is proposed based upon spectroscopic evidence and molecular orbital calculations. The thermal decompositions of 3 and 4 proceed by I_2 evolution at very different rates and lead to different polymorphs of tpp. The mechanism of this process is described in terms of solid state reaction theory.

Introduction

Tpp [2,3,5,6-tetrakis(2′-pyridyl)pyrazine] was synthesized by Goodwin and Lions more than 35 years ago.[1] The molecule has recently attracted interest for its role as a building block in the construction of highly conjugated extended solids. The five heterocyclic rings contain six nitrogen atoms which can act as Lewis bases. Four of these (the pyridyl nitrogens) are very mobile in relation to the other two, leading to a variety of potential coordination modes. This concept has been exploited by us and others in the design of bimetallic complexes[2,3] and polymers[4] in which the metal centers are in electronic communication with adjacent centers *via* the ligand π-system.

The flexibility of the ligand, while useful, presents difficulty in the rational design of extended solids, since it is not always obvious how the ligand will interact with a given Lewis acid. As part of a study of charge-transfer complexes of diazines,[5] we have been forced to examine the rotational energetics of tpp.[6] The ligand has been isolated in two polymorphic forms, crystallizing in either a tetragonal (**1**)[6,7] or a monoclinic (**2**)[6,8] space group, depending upon the solvent system used for crystal growth. The major difference between the two forms involves the orientation of the pyridine rings with regard to the pyrazyl nitrogen atoms. Although each form of the tpp molecule possesses crystallographic C_i symmetry, the tetragonal form has an '*endo*,*exo* conformation' with the nitrogen atoms of adjacent pyridyl rings lying on the same side of the pyrazine ring plane, while the monoclinic form has an '*endo*,*endo* conformation' with nitrogen atoms of adjacent pyridyl rings lying on the opposite sides of the pyrazine ring plane. We have shown that the tetragonal form, **1**, is quantitatively converted to the monoclinic polymorph, **2**, upon heating to 257 °C.[6] In this paper, we examine the influence of iodine coordination on the conformation of tpp. Surprisingly, we find that the formation of simple, metastable, charge transfer complexes can control the ultimate conformation of tpp in the solid state after thermally induced removal of iodine.

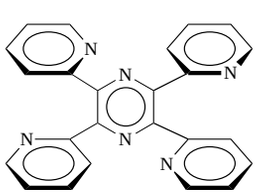

1

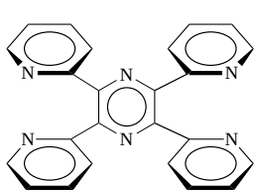

2

Experimental

General

Tpp was purchased from GFS Chemicals, Columbus OH, and was purified by recrystallization from 95% ethanol or toluene. Iodine was purchased from Fisher Scientific Co., Fair Lawn, NJ, and was resublimed prior to use. Solvents were obtained from commercial houses and were dried and purified by standard techniques and stored over activated sieves. Far IR and IR spectra were obtained as Nujol mulls in sealed polyethylene bags on Nicolet 20F and 510 spectrometers, respectively. Carbon, hydrogen and nitrogen analyses were performed by Atlantic Microlabs, Norcross, GA.

X-Ray diffraction

Powder diffraction data were acquired on a Scintag XDS/2000 theta–theta diffractometer with Cu-Kα_1 radiation (λ = 1.540 60 Å) and an intrinsic germanium solid-state detection system. Single crystal intensity data for compound **4** were measured at 21 ± 1 °C by using $\omega/2\theta$ scans (2θ max = 48°) on a Nicolet R3mV diffractometer with graphite-monochromated Mo-Kα radiation (λ = 0.71073 Å). The data were corrected for Lorentz and polarization effects; the intensities of three reflections, remeasured periodically throughout data collection, varied by less than 2%, indicating no need for a decay correction. An absorption correction based on azimuthal scans of several intense reflections, was applied to the data. The structure was solved by direct methods and refined by using full-matrix least-squares techniques. All non-hydrogen atoms were refined anisotropically and all hydrogen atoms were included at idealized positions (d_{C-H} = 0.96 Å) with a refined isotropic group thermal parameter [U_H = 0.07(1) Å^2]. Structure solution, refinement and the calculation of derived results were performed with the SHELXTL[9] package of computer programs. Neutral atom scattering factors and the real and imaginary anomalous dispersion corrections were taken from *International Tables for X-ray Crystallography*, Vol. IV.[10] Relevant crystallographic data are given in Table 1, and selected distances and angles are listed in Table 2.†

† Atomic coordinates, distances and angles and anisotropic displacement parameters have been deposited at the Cambridge Crystallographic Data Centre (CCDC) (reference number 188/99). See 'Instructions for Authors', *J. Chem. Soc.*, *Perkin Trans. 2*, 1997, Issue 1. Any request to the CCDC should give the full literature citation and reference number.

Table 1 Crystal data for **4**

Formula	$C_{24}H_{16}N_6I_4$
M_w	896.05
Crystal system	Monoclinic
Space group	$P2_1/c$ (No. 14)
a/Å	11.842(3)
b/Å	7.804(2)
c/Å	15.243(3)
β/°	95.19(2)
V/Å^3	1402.9(6)
Z	2
D_c/g cm^{-3}	2.12
μ/mm^{-1}	4.42
Transmission coefficient	0.82/1.00
No. obsd data [$I > 3\sigma(I)$]	2064
$R(F_0)^a$	0.0554
$R_w(F_0)^b$	0.0788

^{a} $R = \Sigma||F_o| - |F_c||/\Sigma|F_o|$. ^{b} $R_w = [\Sigma w(|F_o| - |F_c|)^2/\Sigma w(F_o)^2]^{\frac{1}{2}}$

Table 2 Selected bond distances (Å) and angles (°) for **4**

Distances			
I(1)–I(2)	2.750(1)	I(1)–N(2)	2.562(8)
N(1)–C(1)	1.33(1)	N(1)–C(2)	1.34(1)
N(2)–C(3)	1.34(1)	N(2)–C(7)	1.36(1)
N(3)–C(8)	1.34(1)	N(3)–C(12)	1.33(1)
Angles			
I(2)–I(1)–N(2)	173.0(2)	C(1)–N(1)–C(2)	119.3(7)
I(1)–N(2)–C(3)	130.6(6)	I(1)–N(2)–C(7)	111.4(6)
C(3)–N(2)–C(7)	117.9(8)	C(8)–N(3)–C(12)	118.0(9)

Thermal analysis

Thermal gravimetric analyses of tpp·I_2 and tpp·2I_2 were performed on a Perkin-Elmer Series 7 analyser with the TGA7 software package (version 2.20). The samples had a mass of approximately 10 mg each and all calculations were performed on data represented as percent loss of starting mass. For onset calculations, the samples were heated at a constant rate of 5 °C min^{-1} from 25 °C until all of the material had evaporated. Mass loss and onset calculations were performed by standard methods.

Molecular modelling

All calculations were performed on a CAChe Scientific Molecular Modelling workstation. Semi-empirical molecular orbital calculations were performed using the CAChe implementation of MOPAC 6.0 using the PM3 Hamiltonian[11] and standard parameters. Initial geometries for structures **6** and **8** were taken from the X-ray crystal structure **2**, while those of **7** and **9** were taken from the crystal structures of **4** and **1**, respectively. Each was modified by adding I_2 as required and using the N–I, I–I and N–I–I bond lengths and angles found experimentally in

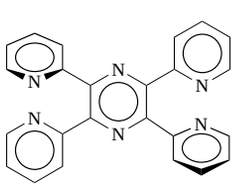

5

structure **4**. Final structures for **6**–**9** were obtained by PM3 geometry optimization using the BFGS minimization strategy.[11b] The structure of **5** was obtained from a MOPAC saddle point calculation as previously reported.[6] The torsional angles in Table 3 were defined by four consecutive atoms, beginning from the pyridyl nitrogen on the ring of interest, through the two carbons involved in the pyrazine–pyridyl bond and finally ending at the adjacent carbon in the pyrazine ring. The torsional angle is the angle observed between the pair of atoms in each ring. The N–N atom distances reported are between the nitrogens of the two pyridine rings on a particular side of the pyrazine ring.

Synthesis of tpp·I_2 3

Method A. In a typical reaction, either tetragonal or monoclinic tpp (0.20 g, 0.51 mmol) was lightly ground and placed in a vial with a slight excess of iodine crystals (0.15 g, 0.59 mmol). The vial was stoppered and sealed with Parafilm. Formation of a reddish-brown powder began immediately. The reaction was monitored by periodically removing small portions for powder diffraction analysis, and was found to be complete in approximately 24 h (typical yield, >95%). Excess of I_2 in the reaction was adsorbed onto the plastic stopper of the sample vial. Changing the I_2/tpp molar ratios to 2, 3 and 4 gave only **3** and excess I_2. For tpp·I_2: ν/cm^{-1}(Nujol) 2900 (s), 1461 (s), 1377 (m), 730 (s). Far IR ν/cm^{-1}(Nujol) 634 (w), 547 (m), 406 (w), 172 (s), 100 (m). Calc. for $C_{24}H_{16}N_6I_2$: C, 44.88; N, 13.09; H, 2.51%. Found: C, 47.07; N, 13.58; H, 2.56% (representative values: the observed deviation in these values is presumably due to loss of I_2 from the sample prior to analysis).

Method B. Diffusion of limited amounts of I_2 into chloroform solution of tpp was also found to give **3**; however, slow evaporation of this solution also gives deeper red crystals of an additional product, identified as tpp·2I_2.

Synthesis of tpp·2I_2 4

Compound **4** is the sole product of diffusion of excess I_2 into a methylene chloride solution of tpp (similar to method B, above). We observe that **4** is also formed from iodine diffusion into hexane and toluene. When ethanol is used as the solvent a complex mixture of polyiodide salts is formed in addition to **4**.[12] For tpp·2I_2: ν/cm^{-1}(Nujol) 2896 (s), 1461 (s), 1377 (m), 730 (s). Far IR ν/cm^{-1}(Nujol) 632 (w), 623 (w), 549 (s), 535 (w), 500 (w), 410 (m), 278 (m), 173 (s). Calc. for $C_{24}H_{16}N_6I_4$: C, 32.17; N, 9.38; H, 1.80%. Found C, 33.03%; N, 9.46; H, 2.03% (the observed deviation in these values is presumably due to loss of I_2 from the sample prior to analysis).

Results

Synthesis of tpp·I_2 (3) and tpp·2I_2 (4)

In solution, the two polymorphic conformations of tpp interconvert rapidly on the NMR timescale.[6] Diffusion of limited amounts of I_2 into a chloroform solution of tpp results in the precipitation of a reddish-brown microcrystalline material, **3**, with the stoichiometry tpp·I_2 (by elemental analysis). If the solvent is allowed to evaporate, a second material is obtained from the highly concentrated mother liquor. This material forms large, deep red crystals with a stoichiometry of tpp·2I_2 (**4**). Higher concentrations of I_2 result in exclusive formation of **4**. Other solvent systems were explored and also found to give **4** with the exception of ethanol, which gives both **4** and unusual polyiodide salts. The salts result from protonation by incipient water and will be discussed in detail elsewhere.[12]

If crystals of either tpp polymorph are exposed to I_2 vapors, 1 : 1 tpp·I_2 complexes are readily formed in a solid-state process. These products give IR spectra and X-ray powder patterns (Fig. 1) that are identical to each other and to **3** grown from solution. Exposure of **3** to additional I_2 does not lead to any further reaction.

Vibrational and thermal analysis of 3 and 4

The IR and far-IR spectra of **3** and **4** are superimposable. The compounds had the expected ring breathing modes, C–H stretches and other characteristic vibrations of a tpp complex. In addition, the far-IR exhibited a strong signal at 172 cm^{-1} which is attributed to the I–I stretching vibration.

Compound **3** loses I_2 readily under ambient conditions, producing exclusively the tetragonal polymorph **1** (as verified by

Table 3 Experimental and calculated dihedral angles and N–N bond distances for compounds **1**, **2** and **4**–**9**[a]

Compound	Torsion angle 1 (°)	Torsion angle 2 (°)	Torsion angle 3 (°)	Torsion angle 4 (°)	N–N dist. 1 (Å)	N–N dist. 2 (Å)	ΔH_f[e]/kcal mol^{-1}
1[a]	46.0	−122.8	122.8	−46.0	3.642	3.642	
2[a]	47.5	50.0	−50.0	−47.5	3.243	3.642	
4[b]	56.1	28.5	−28.5	−56.1	2.982	2.982	257.8
5[c]	94.7	−1.3	4.6	−97.3	3.279	3.318	
6[d]	79.5	55.6	−60.4	−83.0	3.824	3.791	220.5
7[d]	80.9	35.8	−36.4	−79.5	3.514	3.485	221.6
8[d]	72.6	55.7	−60.7	−57.3	3.697	3.425	200.1
9[d]	48.0	−117.4	117.6	−51.3	3.694	3.670	199.1

[a] X-Ray crystal data, ref. 6. [b] X-Ray crystal data, this work. [c] MOPAC calculation, ref. 6. [d] MOPAC calculation, this work. Structures **6** and **7** are rotational isomers of **4**, and **8** and **9** likewise are rotational isomers of **3**. [e] 1 cal = 4.184 J.

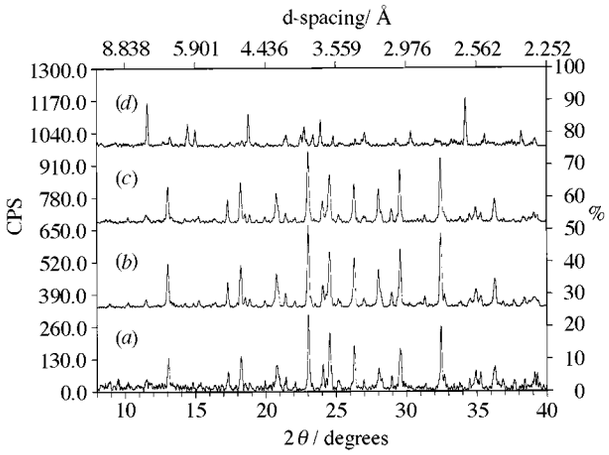

Fig. 1 Powder diffraction spectra for (*a*) tpp·I_2 crystallized from chloroform; (*b*) tpp·I_2 prepared by solid-state reaction using tetragonal crystals; (*c*) tpp·I_2 prepared by solid-state reaction using monoclinic crystals; (*d*) tpp·$2I_2$ crystallized from methylene chloride

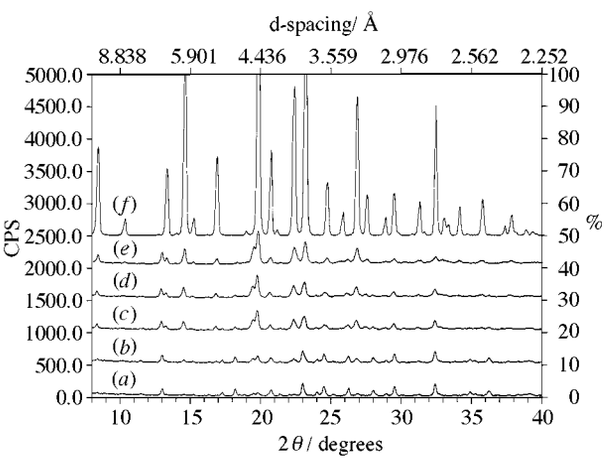

Fig. 2 Powder diffraction spectra of tpp·I_2 monitored over time after being opened to the atmosphere: (*a*) t = 0.0; (*b*) 4 h (*c*) 15 h; (*d*) 17 h; (*e*) 38 h; (*f*) pure tetragonal crystals

powder X-ray diffraction, Fig. 2). This conversion is essentially complete after 24 h at room temperature. Thermal gravimetric analysis shows a single sharp mass loss with an onset temperature of 101.6 °C at a heating rate of 5 °C min^{-1}. In this event, 40% of the total mass is lost, consistent with complete loss of one equivalent of I_2.

In contrast to this, compound **4** loses I_2 very slowly at room temperature. Surprisingly, the product of this decomposition is exclusively the monoclinic polymorph **2** (Fig. 2). The thermal decomposition of **4** is complex and highly dependent upon the physical form of the material. A typical thermogram is shown in Fig. 3. There are two well defined mass losses followed by a slow degradation, prior to vaporization of the tpp matrix. The first event has an onset between 105 and 117 °C and accounts

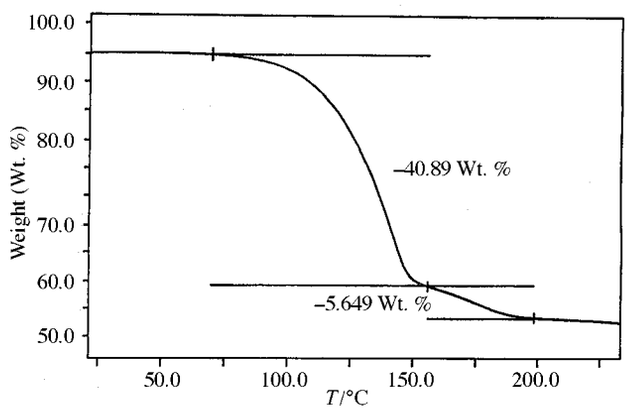

Fig. 3 Thermal gravimetric data for the decomposition of tpp·$2I_2$

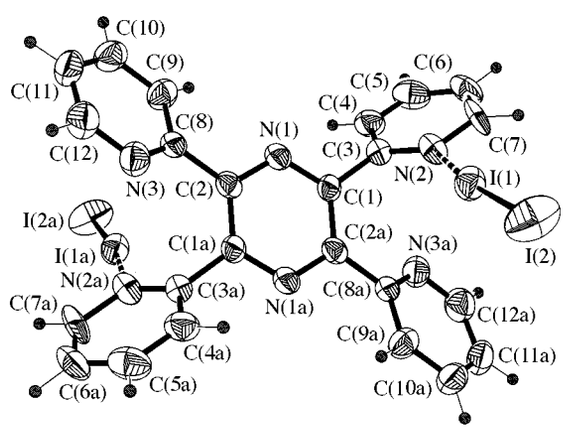

Fig. 4 Thermal ellipsoid plot (50% probability) of tpp·$2I_2$

for 30–42% of the total mass (50–75% of the I_2 in the sample). The second event has an onset of 160–165 °C and accounts for 10–15% of the total mass (17–25% of the I_2). The remainder of the I_2 is lost gradually (not shown in Fig. 2) as the material approaches the melting point of tpp. There is no clear distinction between the loss of the last few percent of the I_2 and the onset of evaporation of tpp (Fig. 3). While thermograms are reproducible for a particular sample batch, there is considerable variation between batches. Each batch was identical by X-ray powder diffraction. No attempt was made to correlate decomposition onset temperatures with particle size.

Structure of tpp·$2I_2$ 4

Tpp·$2I_2$ crystallizes in the space group $P2_1/c$ (No. 14), with two formula units per cell; the asymmetric unit consists of one half of a formula unit situated about an inversion center at (1/2 0 1/2). The complex forms a simple adduct (Fig. 4) with iodine molecules linked to the nitrogen atoms of two inversion related pyridyl rings. As discussed in the previous paper,[13] tpp forms a moderately strong complex with iodine as revealed by the N(2)···I(1) distance of 2.562(8) Å, which is well within

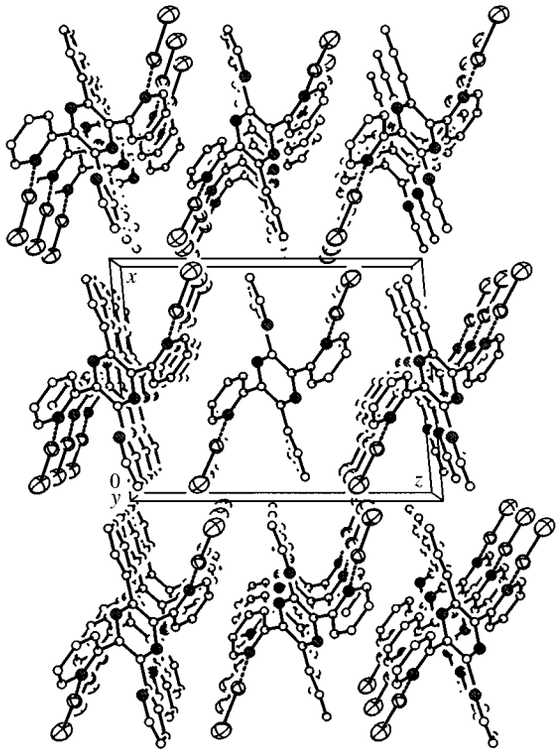

Fig. 5 Crystal packing diagram for tpp·$2I_2$

the sum of van der Waals radii (1.55 Å for nitrogen and 1.98 Å for iodine[14]) and the elongation of the iodine–iodine bond to 2.750(1) Å (*versus* 2.715 Å in elemental iodine[15]). The N···I–I bond angle is slightly bent [173.0(2)°], as is typical of this family of compounds. The bond distances and angles within the tpp moiety are unperturbed by complexation; the values are essentially identical to those observed in either polymorphic form of the compound.[6–8] The ring orientation is very similar to that observed in the monoclinic polymorph; the molecule has an *endo*,*endo* conformation, with nitrogen atoms of adjacent pyridyl rings lying on opposite sides of the pyrazine ring plane. The torsion angle between the pyridyl rings bound to iodine and the central pyrazine ring is 56.1°, and that between the unbound pyridyl rings and the pyrazine ring is 28.5°. Relative to the monoclinic form, the pyridyl rings bound to iodine are rotated by 5.8° toward a more perpendicular orientation with the pyrazine ring, while the unbound pyridyl rings are rotated by 20.0° toward an orientation parallel to the pyrazine ring. This results in a decrease of the N···N distance between the two pyridyl nitrogen atoms from 3.243(4) Å in the monoclinic form to 2.98(1) Å.

There is no evidence of extended interaction between the uncomplexed end of the iodine molecule and any of the available donor sites (Fig. 5). Instead, the packing is dominated by association of the organic and iodine moieties into distinct regions.

Discussion

Structure and decomposition of 4

Charge-transfer complexes between iodine and aromatic nitrogen heterocycles are well known and a substantial body of data has been gathered on the solution equilbria between these complexes and their free components. For example, pyridine initially forms a 1:1 complex with I_2 in which the nitrogen is bound to one end of the iodine molecule with an N–I–I bond angle of approximately 180°.[16] Depending upon conditions, other species can be formed, including salts.[17] Theoretical calculations suggest that at high pyridine concentrations, a 2:1 complex may be formed in which pyridine coordinates to both ends of the iodine.[18] In the solid state, 1:1 complexes between pyridine derivatives and I_2 are the norm (the parent pyridine·I_2 crystal structure has not been reported). Conversely, pyrazine and its derivatives form polymeric structures in which both ends of the iodine are coordinated, as are each of the pyrazine nitrogens.[5]

Multi-ring systems which contain both pyrazine and pyridine components appear to offer the possibility of forming unique extended structures in the solid state. Tpp offers six different nitrogen atoms for potential I_2 coordination, ensuring a high concentration of donor sites. Complexes with tpp:I_2 ratios of either 1:1 or 1:2 can be prepared from solution, with the latter composition favored. The 1:1 adduct has also been prepared in a solid state reaction. In neither case have we found evidence of polymeric structures.

We have previously noted[13] that the more nucleophilic pyridine groups will preferentially coordinate the iodine molecules over less nucleophilic pyrazine groups. The crystal structure of tpp·$2I_2$, **4**, is consistent with this trend. The iodine coordinates to two inversion-related pyridyl rings. Only one end of the I_2 is associated with a nitrogen donor. The organic rings and the halides each condense into distinct channels, prohibiting association of the second iodine atom with any of the other donor sites. The remaining structural features are similar to other pyridine–I_2 complexes. The lack of significant perturbation in N–I bonding means that each coordination site may be regarded as an independent system.

We have noted that the pyridyl rings in the monoclinic tpp polymorph **2** and those in complex **4** are oriented in much the same manner. The nitrogens on each pyridyl ring lie just above or below the plane of the pyrazine and away from the pyrazine nitrogens. Thus, the thermal decomposition of **4** proceeds without substantial change in the ring orientation (Scheme 1).

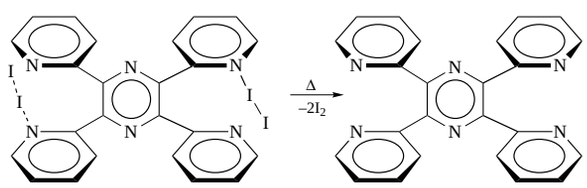

4 **2**

Scheme 1 Thermal decomposition of **4** to give **2**

It also follows that the decomposition of **4** does not proceed through the mono-I_2 complex **3**, which gives exclusively polymorph **1** on thermal decomposition. We have monitored the decomposition of **4** by X-ray diffraction and have observed no other species during the reaction (Fig. 3).

Solid state decompositions involving the evolution of gas are surface phenomena.[19] As I_2 is lost from the surface of a crystal of tpp·$2I_2$ (**4**), a layer of **2** is left behind. While we demonstrated that **2** is able to absorb I_2 from the gas phase (to give tpp·I_2, **3**), transport of iodine across the **4/2** interface does not occur readily. Substantial loss of I_2 results in the sintering of the crystal to form cracks and channels by which I_2 can escape. The TGA data (Fig. 2) of the decomposition indicates that this is not a simple process. At some point, the particles become small enough that the reaction stops due to the surface tension of the insulating layer of **2**. Upon further heating, a second event occurs, but this also stops before all of the iodine is liberated. The thermograms indicate that residual pockets of **4** remain up to the temperature of the melting of the tpp matrix.

Structure and decomposition of 3

The IR and far-IR spectra of tpp adducts **3** and **4** are identical, indicating that they are very closely related compounds. Each has an absorption at 172 cm^{-1}, which is due to the I–I stretching vibration. This vibration is not consistent with pyrazine extended structures, but is typical of pyridine-bound I_2. We have recently shown that such polymeric species typically

have shorter, stronger I_2 bonds which resonate, in Nujol, at wavenumbers ranging from 180 to more than 200.[13]

It is reasonable to conclude that **3** must have a ring orientation much like that of **1** (Scheme 2). Since the decomposition

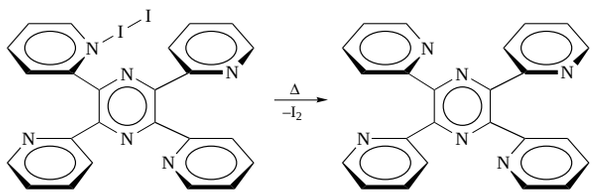

3 **1**

Scheme 2 Proposed structure for **3** and its thermal decomposition to give **1**

of **3** is much more facile than that of **4**, it is unlikely that substantial ring rotation and the accompanying disruption of the crystalline matrix is occurring in this system. Moreover, if the loss of I_2 from **3** involves ring rotation, it is likely that the final product would be **2** rather than the less stable polymorph, **1**. The TGA indicates that all of the iodine in the sample is lost in a single event. As with the decomposition of **4**, we visually observe sintering of the crystal, but inhibition of the decomposition process by the build-up of the decomposition product, **1**, is not observed. We explain this by proposing that I_2 transport across the **3/1** interface is a facile procedure. To a certain extent at least, I_2 is able to diffuse through the matrix of **1**. This proposal also explains the ready formation of **3** from tpp when exposed to I_2. The coordination reaction is not simply the reverse of the decomposition reaction, since formation of **3** begins at the surface and moves inwards, much like the corrosion of a metal. Not only does the process require a mobile **3/1** interface, but it also requires ready diffusion of I_2 through the matrix of **3**. Diffusion through a solid requires point defects or vacancies for the mobile component to slip into.[19] Compound **3** inherently has numerous 'vacancies', since only one side of the complex is coordinated to iodine at any one time. Conversely, compound **4** is saturated with iodine, and diffusion is thereby hindered.

Computational studies

We have investigated the influence of I_2 on the geometry of tpp with molecular orbital calculations. Since MOPAC predicts gas phase behavior, we initially neglect the influence of packing energies on the solid state structure and concentrate on the forces operating within the molecule. The observed structures are then rationalized by considering packing energy contributions. Table 3 shows select experimental atomic distances and torsional angles for structures **1**, **2** and **4**, as well as calculated values for **5**, the reported[6] transition state in the thermal conversion of **1** to **2**.

Table 3 also contains data for calculated gas phase minimum energy conformations of I_2 complexes. Beginning with the experimentally determined geometry of **2**, we added I_2 to two symmetry related pyridyl rings (using the observed N–I and I–I bond distances from **4** as well as the observed N–I–I bond angle). We then optimized the geometry using the standard PM3 Hamiltonian and parameters found in the MOPAC computational method to give structure **6**. When the torsional angles of optimized structure **6** are compared to those of the observed structure, **4**, we find that the I_2-coordinated rings (angles 1 and 3) are twisted out of the ring, as expected, but that the calculations predict a much larger change than is actually observed (calc: *ca.* 81°, obs.: 56.1°). MOPAC predicts that the uncoordinated rings will also be twisted out of the plane of the pyrazine rather than into it as is actually observed (calc: 58°, obs.: 28.5°). If the same minimization calculation is run beginning from structure **4** a slightly different geometry is obtained (**7**). Essentially the same torsional angles are obtained for the I_2-coordinated rings, but the rotations of the non-coordinated rings are far less. The predicted heats of formation of **6** and **7** are quite similar, but are substantially less than that predicted for **4** (Table 3). These results indicate a strong conformational preference for twisting the coordinated rings out of planarity with the pyrazine upon I_2 coordination, thus minimizing N–N and N–I interactions. Once this is done however, the torsional angles of the remaining rings are relatively unimportant to the overall energy. The disparity in the geometries of **4**, **6** and **7** comes about because of packing considerations. In the solid state, efficient packing appears to require compression of the pyridyl rings to enhance π–π stacking interactions. The requirement for efficient packing may also explain why **4** has a structure similar to that of **2** rather than that of **1**.

If **2** is modified by coordination of only a single I_2, and the resulting structure is energy-minimized, structure **8** results. We again observe that the coordinated ring is twisted out of the pyrazine ring plane. The remaining rings are also twisted in the same manner, but to a lesser extent. Conversely, if I_2 is added to an *exo* ring of **1** (**9**), we observe only slight (*ca.* 5°) changes in the various torsional angles. The calculated heat of formation of **9** is also slightly lower than that of **8**. We predict that inherent asymmetry in this system shifts the optimal conformation of **3** to a geometry much like that of **9**, rather than that of **8**. This is because the energy costs of ring compression on packing can be avoided in this geometry, while the costs of I_2 disruption are present in any case. The geometry of **9** is also optimal for the migration of I_2 through the tpp lattice since it can slip between the columns of the organic matrix rather than between the stacked faces.

Exposure of **2** to iodine vapours followed by removal of the iodine source yields only tpp polymorph **1**. This process effects the conversion of a stable polymorph to a metastable one under exceedingly mild conditions. We have previously shown that the simple intraconversion of tpp polymorphs must proceed through an intermediate structure, **5**, in which two, symmetry-related rings rotate perpendicular to the pyrazine ring (and 180° from each other) while the other two rings become co-planar with the pyrazine ring.[6] We have shown in this work that coordination of I_2 to a tpp pyridyl ring (**2**→**4**) twists the complex towards this transition geometry, with the I_2-bearing rings turning out of the plane while the other rings become mobile. This phenomena has previously been noted for addition of HCl to tpp,[8] where the coordinated rings are rotated even further out of the pyrazine plane than in **4**. Thus, the presence of a suitable acceptor seems to facilitate the very geometric changes required for polymorph intraconversion.

References

1 H. A. Goodwin and F. Lions, *J. Am. Chem. Soc.*, 1959, **81**, 6415.

2 (*a*) M. Graf, B. Greaves and H. Stoeckli-Evans, *Inorg. Chim. Acta*, 1993, **204**, 239; (*b*) L. M. Vogler, B. Scott and K. J. Brewer, *Inorg. Chem.*, 1993, **32**, 898; (*c*) A. Escuer, T. Comas, J. Ribas, R. Vicente, X. Solans, C. Zanchini and D. Gatteschi, *Inorg. Chim. Acta*, 1989, **162**, 97; (*d*) R. R. Ruminski, J. L. Kipling, T. Cockroft and C. Chase, *Inorg. Chem.*, 1989, **28**, 370; (*e*) R. R. Ruminski and C. Letner, *Inorg. Chim. Acta*, 1989, **162**, 175; (*f*) R. R. Ruminski and J. L. Kipling, *Inorg. Chem.*, 1990, **29**, 4581.

3 L. W. Morgan, G. J. Shafer, T. W. Hanks, W. T. Pennington and J. D. Petersen, Manuscript in preparation. Syntheses and structural characterization of the following compounds will be reported: $[(H_2O)_2Cu(tpp)Cu(H_2O)_2](ClO_4)_4\cdot H_2O$; $[(H_2O)_2Cu(tpp)Cu(H_2O)_2](ClO_4)_4\cdot 2H_2O$; $[(H_2O)_2Cu(tpp)Cu(H_2O)_2](ClO_4)_4\cdot 2C_2H_5OH$; $[(H_2O)(CH_3CN)Cu(tpp)Cu(H_2O)(CH_3CN)](ClO_4)_4$; $[(H_2O)(NO_3)Cu(tpp)Cu(H_2O)(NO_3)](NO_3)_2\cdot 2H_2O$; $[Cl_2Cu(tpp)CuCl_2]\cdot 5H_2O$.

4 (*a*) L. W. Morgan, K. V. Goodwin, W. T. Pennington and J. D. Petersen, *Inorg. Chem.*, 1992, **31**, 1103; (*b*) K. V. Goodwin, W. T. Pennington and J. D. Petersen, *Acta Crystallogr., Sect. C*, 1990, **46**, 898; (*c*) M. L. Kirk, W. E. Hatfield, M. S. Lah, D. Kessissoglou, V. L. Pecoraro, L. W. Morgan and J. D. Petersen, *J. Appl. Phys.*, 1991, **69**, 6013; (*d*) L. W. Morgan, W. T. Pennington, J. D. Petersen, R. R.

Ruminski, D. W. Bennett and J. S. Rommel, *Acta Crystallogr.*, *Sect. C*, 1992, **48**, 163; (*e*) S. C. Rasmussen, S. E. Ronco, D. A. Mlsna, M. A. Billadeau, W. T. Pennington, J. W. Kolis and J. D. Petersen, *Inorg. Chem.*, 1995, **34**, 821.
5 R. D. Bailey, M. L. Buchanan and W. T. Pennington, *Acta Crystallogr.*, *Sect. C*, 1992, **48**, 2259.
6 R. D. Bailey, M. Grabarczyk, T. W. Hanks, E. M. Newton and W. T. Pennington, *Electronic Conference on Trends in Organic Chemistry* (ECTOC-1), ed. H. S. Rzepa and J. M. Goodman (CD-ROM), 1995, Royal Society of Chemistry publications. See also http://www.ch.ic.ac.uk/ectoc/papers/
7 G. Greaves and H. Stoeckli-Evans, *Acta Crystallogr.*, *Sect. C*, 1992, **48**, 2269.
8 H. Bock, T. Vaupel, C. Nather, K. Ruppert and Z. Havlas, *Angew. Chem.*, *Int. Ed. Engl.*, 1991, **30**, 1678.
9 G. M. Sheldrick, SHELXTL, Crystallographic Computing System, Nicolet Instruments Division, Madison, WI, 1986.
10 *International Tables for X-ray Crystallography*, Vol. IV, The Kynoch Press, Birmingham, England, 1974.
11 (*a*) J. J. P. Stewart, *J. Comput. Chem.*, 1989, **10**, 209 and references therein; (*b*) D. F. Shanno, *J. Opt. Theory Apps.*, 1985, **46**, 87.
12 R. D. Bailey, M. Grabarczyk, T. W. Hanks and W. T. Pennington, manuscript in preparation. Synthesis and structural characterization of the following compounds will be reported: [dpq(H)]I_3/I_2; [dpq(H)]I_3; [tpp$(H)_2$]$(I_3/I_2)_2$; [tpp$(H)_4$]$(I_3)_2(I)_2$.
13 Preceding paper.
14 A. Bondi, *J. Phys. Chem.*, 1964, **68**, 441.
15 F. Bolhuis, P. B. Van Koster and T. Migchelsen, *Acta Crystallogr.*, 1967, **23**, 90.
16 G. K. Vemulapalli, *J. Am. Chem. Soc.*, 1970, **92**, 7589.
17 C. Reid and R. S. Mulliken, *J. Am. Chem. Soc.*, 1954, **76**, 3869.
18 Y. Danten, B. Guillot and Y. Guissani, *J. Chem. Phys.*, 1992, **96**, 3795.
19 (*a*) H. Schmalzried, *Chemical Kinetics of Solids*, VCH, Weinheim, 1995; (*b*) H. Tanaka, N. Koga and A. K. Galwey, *J. Chem. Ed.*, 1995, **72**, 251; (*c*) D. A. Young, *Decomposition of Solids*, Pergamon Press, Oxford, 1966.

Paper 7/00204A
Received 6*th January* 1997
Accepted 12*th July* 1997